INSIGHTS AND IMAGING PHENOTYPES OF TRANSPORTINOPATHY (LIMB GIRDLE MUSCULAR DYSTROPHY TYPE 1F)

C Angelini [1], M Fanin [2], G Cenacchi [3], E Pinzan [1], V Pegoraro [1], E Tasca [1], V Nigro [4]

1. Fondazione Ospedale San Camillo IRCCS (Venice, IT); 2. University of Padua (Padua, IT); 3. University of Bologna (Bologna, IT); 4. TIGEM (Naples, IT).

Objective and Background

To present clinical, muscle imaging, muscle histopathology, ultrastructural and genetic features in a large Italian-Spanish family with LGMD1F. The LGMDs are a heterogeneous group of hereditary disorders with weakness in proximal limb and/or distal muscles. To date 8 autosomal dominant forms of LGMD are known. LGMD1F phenotype is characterized by a great variability, ranging from early onset, with a severe and rapid progression, to milder slow and late-onset forms. The clinical and morphological features of patients with LGMD1F had not yet sufficiently characterized to suggest a specific etiology.

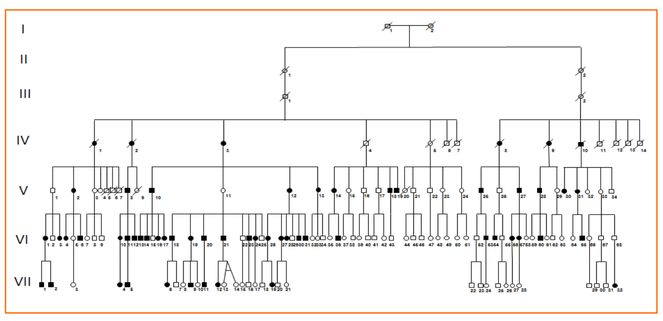

Family pedigree (arrows indicate the two cases investigated).

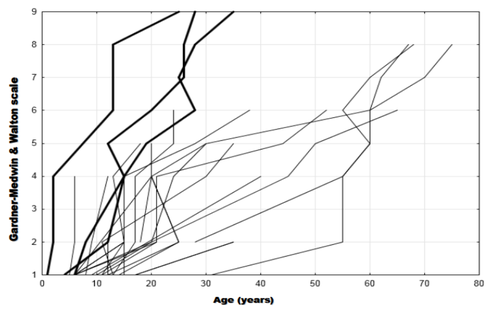

Clinical course in 29 patients. Functional grade assessed using the modified Gardner-Medwin & Walton scale. Rapid course (wheel-chair <30 years, grade=8) in thick line; slow course in thin line.

Design and methods

We collected the clinical history in 19/60 patients and expanded the family pedigree. Muscle biopsy histopathology, immunohistochemistry (desmin, myotilin, p62) and electron microscopy was investigated in one pair of affected patients (mother with 1 biopsy, index patient with 2 biopsies at 9 and 22 years). DNA from 4 patients was studied by Agilent MotorChip CGH array platform to identify the causative gene

Results

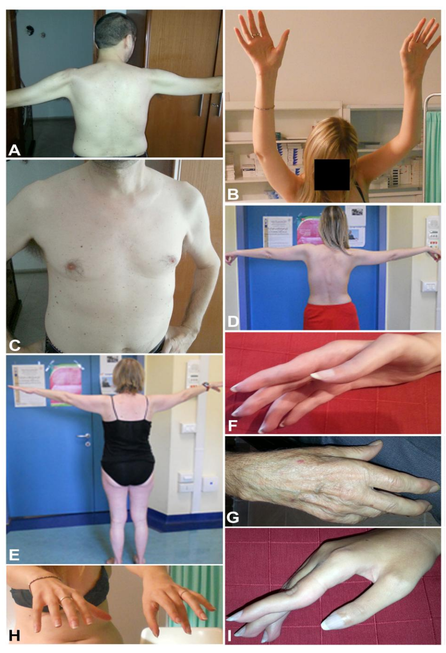

Clinical features of LGMD1F. Note atrophy of upper girdle muscles, especially deltoid and triceps brachii (A-E), scoliosis (D), aracnodattylia (B,F), finger contractures (F,H,I) and atrophy of hand muscles (F,G).

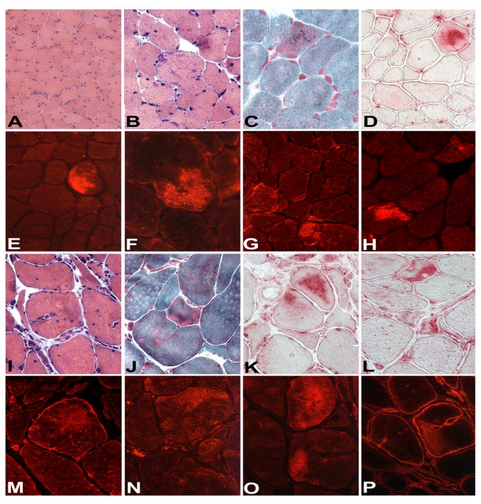

Muscle biopsy histopathology from Case 1 (A-H), and Case 2 (I-P) stained for H&E (A,B,I), trichrome (C,J) acid phosphatase (D,K,L), and immunolabeled for desmin (E,F,G,M,N), myotilin (H,O) and caveolin-3 (P). Case 1 showed a significant reduction of fiber size. Case 2 had prominent chronic changes, such as atrophic fibers, increased central nuclei, and fiber splitting (I,J). Both patients showed fibers with basophilic cytoplasmic areas (B,C,I,J) which reacted for lysosomal acid phosphatase (D,K,L), and had accumulation of cytoskeletal and myofibrillar proteins (E-H,M-O).

Results

Age at onset ranged from 2 to 35 years; in half cases there was hypotrophy both in proximal upper and in lower extremities in calf muscles. We noticed a discrepancy between the clinical severity and muscle biopsy involvement: case 2 has a more severe clinical course and increased muscle fibre atrophy whereas case 1 has a compromised muscle histopathology (more muscle fiber size variability, and autophagic changes). Accumulation of desmin and myotilin and p6-positive aggregates was observed. Electron microscopy revealed accumulation of myofibrillar bodies in muscle fibers. Muscle MRI in case 2 showed selective and severe atrophy in the vastus lateralis muscle.

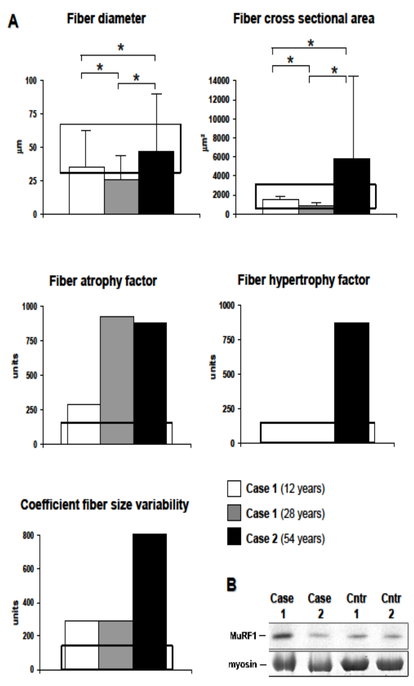

Panel A. Histograms showing the values of different muscle fiber morphometric parameters Dotted rectangles indicate the range of normal values. In Case 1, average fiber diameters were normal but their variability was highly increased. In Case 2, a generalized fiber atrophy was significantly increased in the second biopsy (* = p<0.001). **Panel B. Immunoblot analysis of MuRF-1 protein** in muscle biopsies from controls Case 1 and Case 2. After normalization with myosin protein in the post-transfer Coomassie-stained gel, MuRF-1 quantity was normal in Case 1 (98% of control mean) and highly increased in Case 2 (250% of control mean).

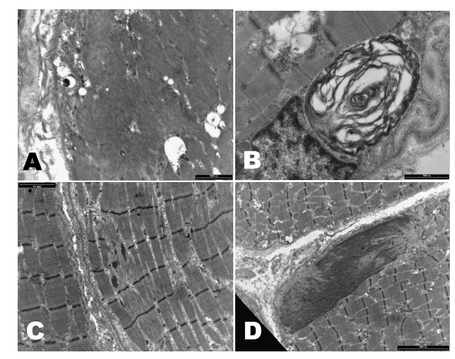

Ultrastructural Analysis. Autophagosomal vacuoles containing cell debris and pseudomyelin figures (A-B), alterations of myofibrillar component, prominent sarcomeric disarray, rod-like structures (C-D) with granular aspect, and occasional cytoplasmic bodies.

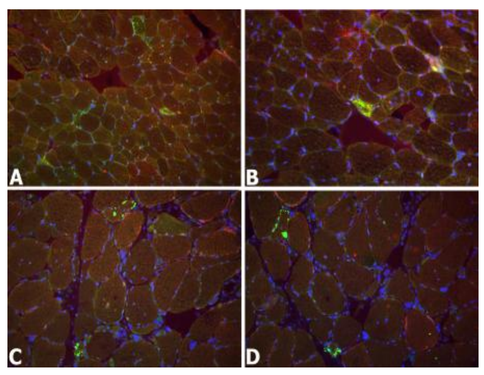

Double immunofluorescence analysis on muscle biopsy sections using antibodies against **p62 (green) and LC3** (red) (counterstain of nuclei with 4′,6-diamino-2-phenylindole, blue) in Case 2 (A,B) and Case 1 (C,D). Note accumulation of p62-positive protein aggregates in some atrophic muscle fibers in both patients.

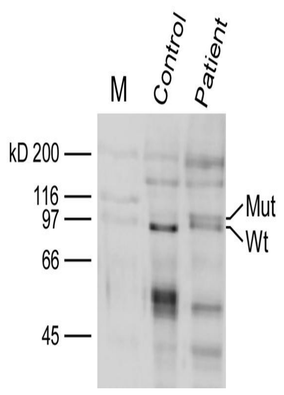

Western blot analysis of skeletal muscle tissue with antibodies to transportin-3 protein (TNPO3). Western blot analysis of skeletal muscle tissue with antibodies to TNPO3. Equal amounts of muscle proteins from a LGMD1F patient and a control were run in each lane and then blotted onto nitrocellulose membrane. A double band is visible in the patient only, due to the effect of a non-spot mutation that causes an enlarged size of the mutant protein as compared to the wild-type protein.

Conclusions

It is possible to hypothesize that the pathogenetic mechanism in LGMD1F might lead to disarrangement of desmin-associated cytoskeletal network. Transportin-3 (TPNO3), which was found to be the causative gene in LGMD1F, is suggest to mediate the nuclear inport-export. The non-stop mutation identified in this family encoded for a longer protein which is expected to be unable to move to the nucleus. Alternatively, it may disrupt the cytoskeletal-nucleus interaction

References

Peterle E, et al. J Neurology 2013 Epub ahead of print
Cenacchi G, et al. Neuropathology 2013 Epub ahead of print
Torella A, et al. PLoS One 8(5): 1-7; 2013

Sin
XLVII CONGRESSO NAZIONALE
22-25 OTTOBRE 2016 – VENEZIA
WebPoster